Micromechanical modelling of twinning-induced plasticity steels

V. Favier[a,*] and D. Barbier[b]

[a] *Arts et Métiers ParisTech, CNRS, PIMM, ENSAM 151 Bd de l'Hôpital, 75013 Paris, France*
[b] *ArcelorMittal Research, Voie Romaine-BP30320, 57283 Maizières-lès-Metz Cedex, France*

Abstract—The paper discusses a number of issues related to the development of a micromechanical polycrystalline model for twinning-induced plasticity steels: twinning features that have to be incorporated, identification procedure, description of the work hardening, role of the texture and the role of the interaction law between grains. Monotonous and reverse strain paths are investigated.

Keywords: Twinning; Work hardening; Mean field analysis; Internal stresses; Strain path change

1. Introduction

Micromechanical modelling and homogenization techniques in mean field approaches are very useful to predict the behaviour for new conditions of loading and to optimize the microstructure of heterogeneous materials providing relevant statistical information about the microstructure and mechanism. In the case of polycrystalline materials such as twinning-induced plasticity (TWIP) steels, homogenization models currently account for the role of the individual grain orientation and of their mechanical interactions. While intergranular stresses are dominant at small strains, the intragranular microstructure changes greatly in the course of the plastic flow and is mainly responsible for the work hardening. TWIP steels submitted to mechanical loading exhibit deformation twins within the grains. These twins act as new barriers to dislocation motion, giving rise the so-called dynamic Hall–Petch effect. Because crystal plasticity modelling successfully describes the stress–strain response and texture development for high stacking fault energy (SFE) cubic polycrystalline materials due to slip alone [1], many studies have tended to introduce twinning in such a framework for low-SFE face-centred cubic (fcc) metals [2,3] considering twinning as a crystallographic shear [4].

The aim of the paper is to report the basic features assumed to be important for modelling of the response of Fe–22Mn–0.6C (wt.%) steel under mechanical loading.

* Corresponding author. E-mail: veronique.favier@ensam.eu

2. Experimental background for Fe–22Mn–0.6C TWIP steel submitted to monotonous loading paths

The main results concerning the mechanical and microstructural responses for two Fe–22Mn–0.6C TWIP steels (2.6 and 15.6 μm grain size) submitted to monotonous loading paths (tension and shear along the rolling RD and transverse directions TD) are recalled and are compared with the modelling in the following sections. When loaded at room temperature, both grain size materials exhibit a high strain hardening in contrast with the strain hardening obtained at 673 K or for high-SFE fcc metals deformed only by crystallographic slip. The main features of the microstructure observed after interrupted tests are recalled. They are common to both grain size materials and to all the loading conditions, unless otherwise stated. More details on these experiments can be found in Refs. [5–9].

(1) Twinning is inhibited during high-temperature deformation (673 K); no twins are visible.
(2) At room temperature and irrespective of the loading path, twins are activated in the earlier stage of deformation, i.e. at $\varepsilon_{eq} = 0.02$.
(3) Grain boundaries are barriers to slip and twinning.
(4) Transmission electron microscopy reveals that twins are organized in bundles composed by several twins 30 nm thick. With increasing strain, the thickness remains constant but the number of twins per bundles increases.

(5) Twins are considered as undeformable hard particles in the austenitic matrix, acting as new obstacles for dislocation motions.
(6) Electron backscattered diffraction analysis reveals that most of the grains exhibit one or two twinning systems for uniaxial tension. The proportion of grains having one twinning system is higher than the one having two twinning systems. The number of grains that do not activate twin systems is higher for the tensile test along the TD than for the RD. In RD simple shear testing, a larger number of grains are only deformed by slip and the twinned grains exhibit one twinning system.
(7) Two active twin systems are sequentially activated in most grains.
(8) In all cases, the volume fraction of twins remains low, i.e. less than 10%.

3. Micromechanical modelling

Grain is considered as the main heterogeneity of the material, consistent with experimental statement (3). A representative volume element (RVE) including 3000 grain orientations was considered to estimate the overall behaviour of the high-Mn TWIP steel polycrystal of interest. The single-crystal constitutive equation is obtained from Ref. [6]; it is based on crystal plasticity and an elastic-viscoplastic approach is adopted. The overall behaviour is deduced by the homogenization scheme, called the translated field model, developed by Sabar et al. [10]. Some twinning features have to be incorporated in representations of single-crystal behaviour. These representations are discussed with regard to the experimental statements recalled above.

3.1. Contribution of both slip and twinning to the inelastic strain and the grain rotation

Following Kalidindi's work [2], the slip contributions to plastic deformation in the untwinned crystal from twinning at the grain scale is depicted. In addition, it was assumed that no slip (and no twinning) occurs in the twinned regions consistent with experimental statement (5). Thus, in a small strain setting, the viscoplastic strain rate can be obtained by the volume average of the viscoplastic strain rate in the matrix and the twinned regions:

$$\dot{\varepsilon}_{ij}^{vp} = \left(1 - \sum_{h}^{N^{(h)}} f^{(h)}\right) \sum_{g}^{N^{(g)}} R_{ij}^{(g)} \dot{\gamma}^{(g)} + \sum_{h}^{N^{(h)}} R_{ij}^{(tw)(h)} \dot{f}^{(h)} \gamma^{tw} \quad (1)$$

where $R_{ij}^{(g,tw)}$ is the Schmid tensor associated with either the slip systems or the twinning ones, where $\dot{\gamma}^{(g)}$ is the slip rate of the system (g), $f^{(h)}$ denotes the volume fraction of the twinned regions associated with the system (h), γ^{tw} is the (constant) shear rate associated with twinning, and $N^{(s)}$ and $N^{(h)}$ represent the number of potentially active slip and twin systems, respectively. In addition, the rotation of the grains was assumed to be only due to slip. The role of twinning was neglected since the twin volume fraction remains low (see experimental statement (8)).

Eq. (1) combines two strain mechanisms: a viscous or rate-dependent mechanism related to thermally activated slip associated with $\dot{\gamma}^{(g)}$ as variable processes (Eq. (2)) and a rate-independent mechanism due to twinning associated with $\dot{f}^{(ht)}$ as variable processes (Eq. (3)). However, to easily couple both inelastic strain mechanisms and for easier numerical handling, a viscoplastic framework is utilized to describe the twin volume fraction rates as is classically done for plasticity by slip alone [1]. The flow rules for both strain mechanisms are written:

$$\dot{\gamma}^{(g)} = \dot{\gamma}_0 \left(\frac{\tau^{(g)}}{\mu}\right)^2 \exp\left(-\frac{\Delta G_0}{kT}\left(1 - \left(\frac{\left|\tau^{(g)}\right|}{\tau_r^{(g)}}\right)\right)\right) sign\left(\tau^{(g)}\right), \quad (2)$$

where $\dot{\gamma}_0$ is a reference slip rate, μ is the elastic shear modulus, ΔG_0 is the activation energy required to overcome an obstacle without any help of stresses (when $\tau = 0$), T is the absolute temperature, k is the Boltzman constant, and $\tau_r^{(g)}$ is a reference shear stress that describes the average resistance of the short- and medium-range obstacles at 0 K and consequently evolves with the strain-hardening state. For $x > 0$, $sign(x) = +1$ and for $x < 0$, $sign(x) = -1$.

Concerning twinning:

$$\text{if } \tau^{tw(h)} \le \tau_c^{tw(h)} \text{ then } \dot{f}^{(h)} = 0 \quad (3)$$

$$\text{if } \tau^{tw(h)} > \tau_c^{tw(h)} \text{ then } \dot{f}^{(h)} = \dot{f}_0 \left(1 - \sum_{t=1}^{12} f^{(t)}\right) \left(\frac{\tau^{tw(h)}}{\tau_c^{tw(h)}}\right)^m$$

where $\dot{f}_0$ is the twinning rate reference, $\tau_c^{tw(h)}$ represents the critical shear stress for twinning, and $1/m$ is the material rate sensitivity.

3.2. Competition between slip and twinning as deformation modes

Regarding experimental statements (1), (2) and (6), slip and twinning are competitive deformation processes depending on temperature and loading path. The latter is closely related to the anisotropy of both mechanisms and should be inherent to the modelling provided the texture evolution is well described. Temperature dependence is much more complex and affects different aspects of the mechanisms. Concerning slip, perfect dislocation glide is mostly thermally activated because thermal assistance is required here in order to overcome obstacles having low activation energy such as solute atoms. Consequently, the flow stress decreases with increasing temperature. In addition, the strain-hardening behaviour is also temperature sensitive since the dynamic strain aging is stronger with increasing temperature [11]. The temperature dependence of deformation twins is known to be related to SFE. A high SFE inhibits deformation twins and consequently promotes usual slip [12]. The temperature dependence for slip is associated with kinetic aspects leading to both thermal and strain-rate sensitivity. However, twinning is often treated as a phase transformation process with moving boundaries and is thus analyzed by applying pure energy considerations [3]. In the present modelling, a similar idea was followed. The temperature dependence for

twinning is captured via the value of the critical shear stress for twinning (Eq. (3})) while for slip, it is directly incorporated in the flow rule (Eq. (2)). Consequently, decreasing the temperature (1) reduces thermally assisted slip and/or (2) promotes twinning by decreasing SFE. Despite some works dedicated to the transition from slip-dominated to twinning-dominated deformation mechanisms for body-centred cubic (bcc) and hexagonal close-packed (hcp) material subjected to high strain rates [13,14], the coupling between effects (1) and (2) is still under discussion for fcc metals. The competition between slip and twinning depends also on how both mechanisms are affected by work hardening. This is the purpose of the next section.

3.3. Additional and anisotropic hardening due to twinning

The coupling between slip and twinning is captured by modelling the reduction of the dislocation mean free path (MFP) due to the increasing number of twins. The evolution of the total dislocation density $\dot{\rho}^{(g)}$ for a slip system (g) accounts for the storage and the dynamic recovery of dislocations and can be written as [15]:

$$\dot{\rho}^{(g)} = \frac{1}{b}\left(\frac{1}{L^{(g)}} - \beta\rho^{(g)}\right)\left|\dot{\gamma}^{(g)}\right| \tag{4}$$

where β is a parameter associated with the dynamic recovery assumed constant with temperature as a first approximation. In the first term $L^{(g)}$ represents the mean free path of dislocations which can be calculated with a harmonic mixing law accounting for the obstacles to dislocation motion. This concept provides a natural setting for, in addition to the dislocation–dislocation interactions and grain boundaries usually considered, the incorporation of twins as barriers to dislocation motion. In the present modelling, the dislocation mean free path is thus determined by:

$$\frac{1}{L^{(g)}} = \frac{1}{D} + B_{gh}\frac{f^{(h)}}{2re(1-\sum_{h=1}^{12} f^{(h)})} + \frac{\sqrt{\sum_{i\neq g}\rho^{i}}}{k} \tag{5}$$

The indexes g and h are associated with the slip and twin systems respectively. D is the effective grain size, K is a parameter to be adjusted and the second term on the right-hand side represents the spacing between the twins secant to the slip system (g). Its expression accounts for the twin organization in stacks where r is the mean number of microtwins per stack and e is the mean thickness of microtwins (see experimental statement (4)). Finally the reference shear stress is written for a multiple system approach:

$$\tau_r^{(g)} = \tau_{r0}^{(g)} + \alpha\mu b\sqrt{\sum_h a^{(gh)}\rho^{(h)}} \tag{6}$$

The increase in twinning resistance is assumed to be due only to twin–twin interaction. The influence of slip is much smaller and so is neglected. The increase in the twinning resistance thus is represented following the law proposed by Kalidindi [2]:

$$\dot{\tau}_c^{tw(t)} = \underbrace{h_{ncp}^{tw}\left(\sum_{t=1}^{12} f^{(t)}\right)^{\alpha}\underbrace{\sum \gamma^{tw}\dot{f}^{(k)}}_{K\in\, non-coplanar\ twin\ system\ with\ h}}_{\text{Term non coplanar}} + \underbrace{h_{cp}^{tw}\left(\sum_{t=1}^{12} f^{(t)}\right)\underbrace{\sum \gamma^{tw}\dot{f}^{(k)}}_{K\in\, coplanar\ twin\ system\ with\ h}}_{\text{Term coplanar}} \tag{7}$$

where α, h_{ncp}^{tw} and h_{cp}^{tw} are parameters that have to be adjusted. Although it is empirical, the main advantage of Eq. (7) is that it accounts for twin–twin interactions and distinguishes between coplanar and non-coplanar twin systems. Furthermore, as Kalidindi [2] claims, it is required to capture the twinning sequential activity [6].

3.4. Stress redistribution within a grain due to the presence of deformation twins

Internal stresses due to twinning are certainly important and lead to a Bauschinger effect (BE) (also termed back-stress) [16,17]. For simplicity, the internal stresses within a grain due to twinning are not considered here.

Concerning the intergranular stresses, accounting properly for the interaction of the grains with their surroundings is of the utmost importance. The classical Taylor model, assuming the hypothesis of equal strain or here strain rate in every grain is known to give a good description of texture development in low SFE fcc metals [4] and hcp metals [18]. However, it results in an extremely rigid interaction because it describes pure elastic interactions. Sabar et al. [10] developed an interaction law which successfully represents the elastic-viscoplastic interactions between grains. This model, termed the translated field model, is inspired by the self-consistent approximation. The interaction law for the translated field model is written as:

$$\dot{\sigma} = \dot{\Sigma} - \mathrm{C} : \left(\mathrm{I} - \mathrm{S}^{\mathrm{E}}\right) : \left(\dot{\varepsilon}^{\mathrm{vp}} - \mathrm{A}^{\mathrm{Be}} : \dot{\mathrm{E}}^{\mathrm{vpe}}\right) \tag{8}$$

where $\dot{\Sigma}$ is the macroscopic stress rate, I is the identity tensor and S^{E} is the elastic Eshelby tensor; A^{Be} is the localization tensor of the viscoplastic strain rate calculated by the self-consistent approximation associated with a pure viscoplastic heterogeneous problem; and $\dot{E}^{vpe}$ is the overall viscoplastic strain rate equal to the average of the local viscoplastic strain rate over the RVE for elastic homogeneous materials, i.e. $\dot{E}^{vpe} = \overline{\dot{\varepsilon}^{vp}}$. Further details can be found in Sabar et al. [10]. The spin tensor concentration relation is expressed as:

$$\dot{\omega} = \dot{\Omega} \tag{9}$$

where $\dot{\omega}$ and $\dot{\Omega}$ are the local and macroscopic spin tensors, respectively.

4. Results and discussion

4.1. Strain-hardening behaviour under monotonous loading

Many experiments performed on low-SFE fcc metals [12,19] have demonstrated that the strain-hardening rate $d\sigma/d\varepsilon$ exhibits a plateau at intermediate strain levels, while, for high-SFE fcc metals (that deform only by slip), $d\sigma/d\varepsilon$ decreases continuously with increasing strain. As far as TWIP steels are concerned, the plateau comprises an increase followed by a decrease rather than a constant value of $d\sigma/d\varepsilon$. The magnitude of this increase and decrease depends on the mean grain size (cf. Figs. 1a and 2) and on a monotonous loading direction (Fig. 1a). This noticeable strain-hardening rate is commonly attributed to the reduction in the dislocation mean free path (MFP) with the twin boundaries acting as obstacles to dislocation glide. However, different interpretations exist concerning the occurrence of this apparent grain-refinement effect (the so-called dynamic Hall–Petch effect). For low-SFE fcc metals under simple and plane compression [19] and simple tension [7], the latter appears at the onset of deformation twinning. But for simple shear, Kalidini and co-workers [19] claim that the primary twin system is mainly coplanar to the primary slip systems and therefore is ineffective at hardening them. This hypothesis should be further investigated.

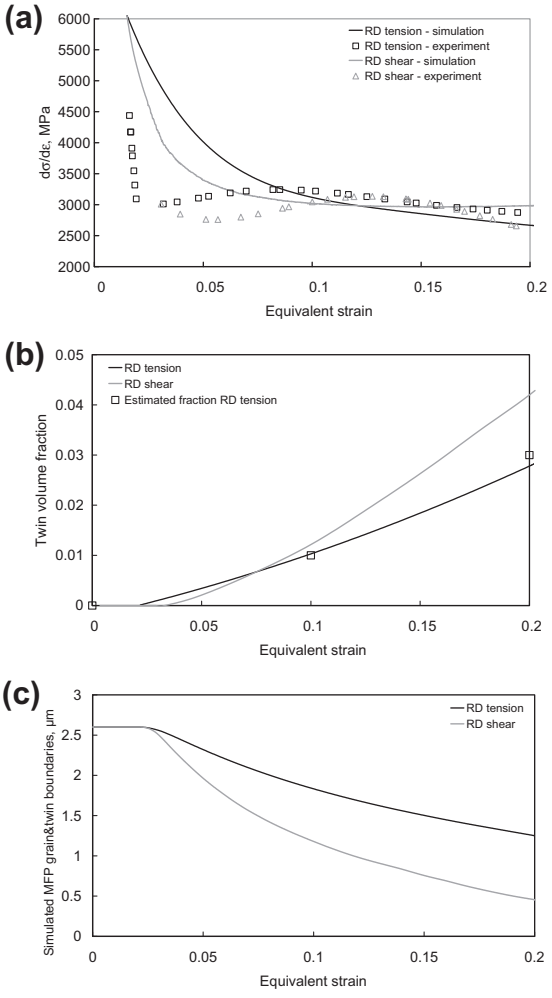

Figure 1. Behaviour and microstructural evolution related to the Fe–22Mn–0.6C TWIP steel with 2.6 μm grain size deformed in RD tension and shear: (a) predicted and experimental strain hardening; (b) predicted and estimated twin volume fraction according to the experimental method developed in Ref. [14]; (c) predicted dislocation mean free path due to grain and twin boundaries.

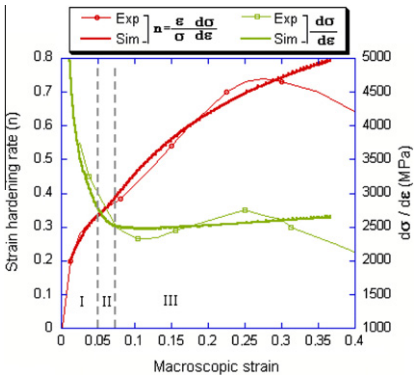

Figure 2. Predicted and experimental evolution of strain hardening in RD tension for the Fe–22Mn–0.6C TWIP steel with a 15.6 μm grain size.

Predicted and experimental strain-hardening curves for RD tension and simple shear are plotted in Figure 1a. They correspond to the Fe–22Mn–0.6C steel with 2.6 μm grain size. In addition, the predicted evolution of the overall twin volume fraction and the dislocation mean free path are plotted as a function of macroscopic equivalent strain (Fig. 1b and c). The x-axes of the graphs in Figure 1 are scaled identically to show the relation between the evolution of the microstructure and the strain-hardening behaviours. The discussion is restricted to small and moderate strains (<0.15) since the modelling is formulated using the small strain hypothesis.

The model predicts a strong decrease in $d\sigma/d\varepsilon$ which significantly slows down with increasing strain to reach either a plateau in the case of RD simple shear loading or a progressive and slight decrease in the case of RD tensile loading. Predicted $d\sigma/d\varepsilon$ is found to be higher for RD tensile loading than for RD simple shear at small strains but becomes closer at moderate strains ($\sim$0.12). These results are consistent with experiments. The slowing down of the decrease in $d\sigma/d\varepsilon$ is associated with the occurrence of twinning and the resulting reduction of the dislocation MFP, though this is delayed (Fig. 1). Indeed, MFP reduction due to twinning starts at 0.02 strain, whereas the stop of the strong decrease in $d\sigma/d\varepsilon$ occurs at 0.05 strain for RD simple shear loading.

Despite the qualitative agreement, the increase and the subsequent decrease of $d\sigma/d\varepsilon$ are not reproduced by the model. Rather, the latter predicts a monotonous $d\sigma/d\varepsilon$ variation. Using the same modelling but applying it to Fe–22Mn–0.6C TWIP steels with a larger mean grain size (and also different fitted model parameters [6]), the origin of the strain-hardening behaviour was investigated in detail. Figure 2 shows the polycrystal work-hardening curve obtained for RD tensile loading.

As in the case of small grain size, an increase followed by a decrease of $d\sigma/d\varepsilon$, which again is not captured by the modelling, is observed. The response at the grain scale was then investigated. Figure 3a represents the strain-hardening curve of a grain selected because its behaviour is representative of most of the grain behaviour in the studied polycrystal. As expected, the first stage of the curve is associated with a strong decrease in $d\sigma/d\varepsilon$. The following stage is associated with the onset of a primary twin system at 0.06 of local viscoplastic strain (Fig. 3b). As a consequence, the dislocation MFP instantaneously decreases since this primary twin system was found to be non-coplanar with the active slip systems. However, Figure 3 clearly shows that this additional MFP reduction does not entail a stop of $d\sigma/d\varepsilon$ decrease. On the contrary, a drastic fall of $d\sigma/d\varepsilon$ is observed as soon as twinning occurs. This effect is attributed to the fact that twinning supplies an additional deformation and "relaxes" intergranular stresses through the localization relation (Eq. (8)). In other words, this latter effect is not immediately balanced by the additional dislocation MFP reduction due to the occurrence of primary twins.

The effects observed at the grain scale cannot be straightforwardly expressed at the polycrystal scale probably because of the averaging procedure used to obtain the overall response from the grain ones and due to the fact that not all the grains display the same behaviour at the same time. However, it explains the delay between the occurrence of the additional dislocation MFP reduction due to twinning and the end of the strong $d\sigma/d\varepsilon$ decrease in the polycrystal response. Nevertheless it underlines the question of the role of the interaction law in the grain and polycrystal responses.

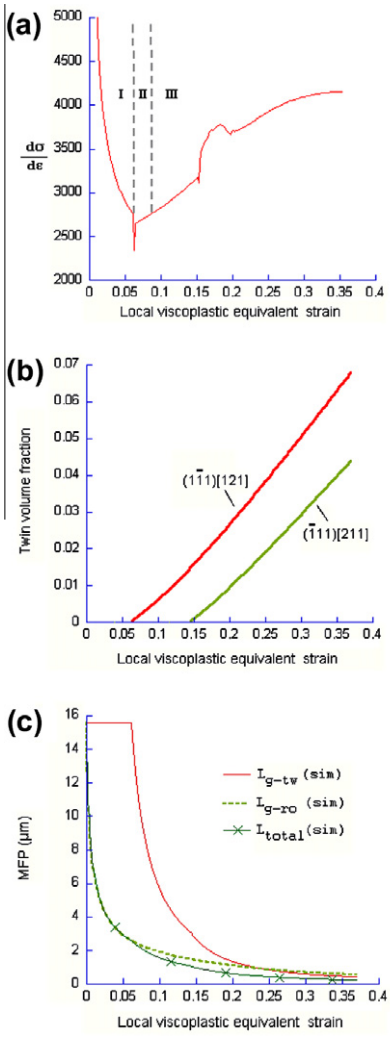

Figure 3. Predicted evolution of different variables of a selected grain of the Fe–22Mn–0.6C TWIP steel with 15.6 μm grain size: (a) strain hardening; (b) twin volume fraction of active twin systems; (c) dislocation MFP due to different obstacles (forest dislocations L_{g-ro}, grain and twin boundaries L_{g-tw} and both contributions L_{total}).

4.2. Interaction law

Materials having such elastic-viscoplastic behaviour display space-time couplings, described by Suquet [20] as a long memory effect. The translated field model used here is highly suited to describing the elastic-viscoplastic nature of the mechanical interactions between grains [10]. On the other hand, however, it delays the mechanical interactions between grains and can be also responsible for the non-expression of the non-monotonous strain-hardening curve at the grain scale to the polycrystal scale.

The question of the interaction law also raises the issue of model parameter identification. Here, most of parameters are physically based. Some of them, such as microstructural parameters (D, r, e) or elastic properties, are deduced directly from experiments. Some physical parameters, such as b, ΔG_0, SFE and ρ_0, are obtained from the literature. Other parameters have, however, been determined to match experimental and calculated data. The identification procedure for this second sort of parameter used data obtained at the polycrystal scale. To be reliable, it must be based on mechanical but also microstructural data. More details on the identification procedure can be found in Refs. [6,9]. Development of micromechanical techniques to measure stress fields using Kossel [21], Kikuchi [22] or Laue microdiffraction diagrams [23], in addition to measurement techniques for kinematic fields, will clearly be of great interest for a direct determination of the local constitutive relation at the local (micron) scale, a necessary step for giving micromechanical models the status of quantitative predictive tools.

4.3. Texture

The present model qualitatively reproduces the anisotropy in the stress–strain and strain-hardening curves, and in twin volume fraction evolution, revealing the significant role of the texture on the overall response for Fe–Mn–C steels. Assuming that twinning does not significantly affect the texture development, Barbier et al. [9] found that the predicted texture is in quantitative good agreement with experiments for all the loading paths. These results demonstrate that the texture of deformed Fe–22Mn–0.6C is slip-dominated. In addition, they found that the predicted twinning activity is consistent with experiments for RD simple shear and TD tension despite the model parameters being fixed by curve-fitting on RD tension curves. Because of the texture, RD

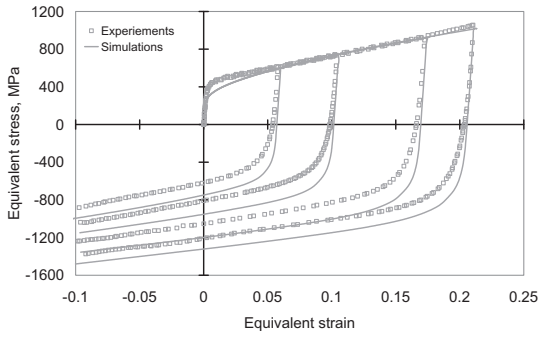

Figure 4. Experimental and predicted curves for the Fe–22Mn–0.6C TWIP steel with a 2.6 μm grain size for the Bauschinger tests at different levels of pre-strain under RD simple shear.

uniaxial tension promotes twinning in 90% of grains and 30% of grains have two active twin systems at 0.07-0.08 strain. Conversely, RD simple shear promotes single twinning in 95% of grains. Twin–twin intersections increase the difficulty of producing new twins, resulting in a lower twin volume fraction for RD uniaxial tension than for RD simple shear. That is the reason why the dislocation MFP reduction is higher in the case of RD simple shear than in the case of RD uniaxial loading (Fig. 2c). Accordingly, the strain-hardening parameter, which was initially lower for RD simple shear than for RD uniaxial tension (as classically found for fcc metals deforming only by slip [24]), increases more quickly with increasing strain to reach the same value as measured for RD uniaxial tension at 0.12 equivalent strain. The present model reproduces this phenomenon quite well mainly because it is closely related to the anisotropic plastic behaviour of the grains and to the texture evolution properly accounted for in the modelling.

4.4. Role of internal stresses—analysis of the responses under non-monotonous loading paths

From the parameter identification on monotonous simple shear deformation, reverse simple shear deformation has been simulated at different pre-strain levels and compared to the experimental curves. The results are presented in Figure 4. During the reverse deformation, the model overestimates the flow stress, i.e. underestimates the BE. By using a translated field approach for the interaction law, the prediction of the intergranular stresses is insufficient to estimate the flow stress of TWIP steels during reverse loading. The intragranular stresses should be explicitly introduced in the model through the description of dislocation pile-up at twin boundaries.

5. Conclusions

We have outlined a point of view for the development of a micromechanical model as a predictive tool of mechanical and microstructural response of TWIP steels. This point of view was substantiated with regard to experimental findings for both establishing and assessing the modelling. The identification procedure has to be conducted on both mechanical and microstructural responses to capture the physical deformation and hardening mechanisms for different monotonous loading paths. However, experimental data have been obtained from tests performed on polycrystalline material. As a result, it depends on the selected interaction law. It is shown that the interaction law induces the single-crystal response as well as the polycrystal one. Texture plays a key role in twinning activity and kinetics. For reverse loadings, intragranular stresses should be taken into account to capture the BE observed in Fe–22Mn–0.6C TWIP steels.

References

[1] S. Paquin, V. Berbenni, X. Favier, M. Lemoine, Berveiller, Int. J. Plast. 17 (2001) 1267.
[2] S.R. Kalidindi, Int. J. Plast. 17 (2001) 837.
[3] M. Cherkaoui, Philos. Mag. V 83 (2003) 3945.
[4] P. Van Houtte, Acta Metall. 26 (1978) 591.
[5] S. Allain, J.P. Château, J.P. Dahmoun, O. Bouaziz, Mater. Sci. Eng. A 387–389 (2004) 272.
[6] M.N. Shiekhelsouk, V. Favier, K. Inal, M. Cherkaoui, Int. J. Plast. 25 (2009) 105.
[7] D. Barbier, N. Gey, N. Bozzolo, S. Allain, M. Humbert, J. Microscopy-Oxford 235 (2009) 67.
[8] O. Bouaziz, S. Allain, C.P. Scott, P. Cugy, D. Barbier, Curr. Opin. Solid State Mater. Sci. 15 (2011) 141.
[9] D. Barbier, V. Favier, B. Bolle, submitted.
[10] H. Sabar, M. Berveiller, V. Favier, S. Berbenni, Int. J. Solids Stuct. 39 (2002) 3257.
[11] U. Essmann, H. Mughrabi, Phil. Mag. 40 (1979) 731.
[12] L. Rémy, Acta Metall. 26 (1978) 443.
[13] B. Plunkett, O. Cazacu, R.A. Lebensohn, F. Barlat, Int. J. Plast. 23 (2007) 1001.
[14] I.J. Beyerlein, C.N. Tomé, Int. J. Plast. 24 (2008) 867.
[15] U.F. Kocks, H. Mecking, Prog. Mater. Sci. 48 (2003) 171.
[16] O. Bouaziz, S. Allain, C. Scott, Scripta Mater. 58 (2008) 484.
[17] I. Gutierrez-Urrutia, J.A. del Valle, S. Zaefferer, D. Raabe, J. Mater. Sci. 45 (2010) 6604.
[18] A.A. Salem, S.R. Kalidindi, S.L. Semiatin, Acta Mater. 53 (2005) 3495.
[19] E. ElDanaf, S.R. Kalidindi, R.D. Doherty, Int. J. Plasticity 17 (2001) 1245.
[20] P. Suquet, in: E. Sanchez-Palencia, A. Zaoui (Eds.), Homogenization Techniques for Composite Media, Springer-Verlag, Berlin, 1985, pp. 193–278.
[21] C. Maurice, R. Fortunier, J. Microscopy–Oxford 230 (2008) 520.
[22] A.J. Wilkinson, D. Randman, Phil. Mag. 90 (2010) 1159.
[23] R. Spolenak, W.L. Brown, N. Tamura, A.A. MacDowell, R. Celestre, H. Padmore, Phys. Rev. Lett. 90 (2003) 6102.
[24] A.B. Lopes, F. Barlat, J.J. Gracio, J.F. Ferreire Duarte, E.F. Rauch, Int. J. Plast. 19 (2003) 1.